Limnol. Oceanogr., 51(2), 2006, 936–949

Phytoplankton photoacclimation and photoadaptation in response to environmental gradients in a shelf sea

C. Mark Moore[1]
National Oceanography Centre, European Way, Southampton SO14 3ZH, United Kingdom

David J. Suggett
Department of Biological Sciences, University of Essex, Colchester CO4 3SQ, United Kingdom

Anna E. Hickman, Young-Nam Kim, and Jacqueline F. Tweddle
National Oceanography Centre, European Way, Southampton SO14 3ZH, United Kingdom

Jonathan Sharples
Proudman Oceanographic Laboratory, Bidston Observatory, Birkenhead CH43 7RA, United Kingdom

Richard J. Geider
Department of Biological Sciences, University of Essex, Colchester CO4 3SQ, United Kingdom

Patrick M. Holligan
National Oceanography Centre, European Way, Southampton SO14 3ZH, United Kingdom

Abstract

Variability in the photosynthetic performance of natural phytoplankton communities, due to both taxonomic composition and the physiological acclimation of these taxa to environmental conditions, was assessed at contrasting sites within a temperate shelf sea region. Physiological parameters relating to the structure of the photosystem II (PSII) antenna and processes downstream from PSII were evaluated using a combination of fast repetition rate fluorescence, oxygen flash yields, spectral fluorescence, and ^{14}C photosynthesis versus irradiance measurements. Parameters relating to PSII antenna structure, specifically the functional absorption cross-section (σ_{PSII}) and the chlorophyll to PSII reaction center ratio, varied principally as a result of spatial (horizontal) taxonomic differences. Phenotypic plasticity in the size of the PSII light-harvesting antenna appeared to be limited. In contrast, parameters related to electron transport rates (ETRs) downstream of PSII, including the maximum ETR ($1/\tau_{PSII}$), the chlorophyll-specific maximum rate of carbon fixation (P^*_{max}), and the light-saturation intensity (E_k), all decreased from the surface to the subsurface chlorophyll maximum (SCM) in stratified waters. The primary photoacclimation response to the vertical light gradient thus resulted in decreasing light-saturated carbon fixation per reaction center with increasing depth. Increases in the ratio of PSII reaction centers to carbon fixation capacity thus dominated the phenotypic response to decreased irradiance within the SCM. Perhaps counterintuitively, phytoplankton populations within fully mixed water columns, characterized by low mean irradiance, were acclimated or adapted to relatively high irradiance.

Photoacclimation describes the phenotypic response of algae to changes in irradiance at the organism level (Falkowski and LaRoche 1991) and can be assessed by measuring differences in the photosynthetic physiology or biochemistry of a given taxon (genotype) in response to growth at a range of light intensities. Photoacclimation involves compensatory changes in a number of components of the photosynthetic apparatus (see reviews by Falkowski 1980; Falkowski and LaRoche 1991; MacIntyre et al. 2002). In particular, acclimation to increased irradiance is typically accompanied by a decrease in cellular photosynthetic pigment content across all taxa (MacIntyre et al. 2002).

In contrast, photoadaptation describes the genotypic response of algae to irradiance that has arisen during evolution (Falkowski and LaRoche 1991). Photoadaptation can be assessed by measuring differences in photosynthetic physiology or biochemistry of different taxa (different genotypes) when grown under identical environmental conditions. At the ecological level, species-specific traits influence the photosynthetic performance of phytoplankton via interactions between the community of genotypes and the environment (Richardson et al. 1983; Cullen and MacIntyre 1998).

[1]Present address: University of Essex, Colchester C04 3SQ, United Kingdom (cmmoore@essex.ac.uk).

Acknowledgments

We thank E. Le Floch, G. Harris, M. Lucas, H. Thomas, and G. Tilstone for assistance with data collection at sea and M. Zubkov for assistance with the flow cytometry analysis. S. Laney kindly provided software and contributed to many useful discussions on the analysis of raw FRR fluorometer data. We also thank the officers and crew of the RRS *James Clark Ross* for their assistance during cruise JR98. Insightful comments from J. Cullen and an anonymous reviewer considerably improved an earlier version of this manuscript.

This work was supported by the Natural Environment Research Council, UK (NER/A/S/2000/01237 to R.J.G.) and (NER/A/S/2001/00449 to P.M.H./J.S.).

Distinguishing between photoacclimation and photoadaptation is important for understanding the mechanisms that regulate primary production in natural communities (Richardson et al. 1983; Cullen and MacIntyre 1998). A better knowledge of the environmental factors that influence the functional relationship between photosynthesis and irradiance (the *P* vs. *E* curve) in natural communities is also needed for improving estimates of oceanic productivity (Behrenfeld et al. 2004). Specifically, ascribing changes in the *P* versus *E* relation to physiological mechanisms or adaptive variability underlies our ability to predict aquatic production under altered environmental forcing (Richardson et al. 1983; Cullen and MacIntyre 1998; MacIntyre et al. 2002).

The response of the molecular structure of the photosynthetic apparatus to changing irradiance varies between species (Fig. 1). Some taxa can acclimate to decreased irradiance by increasing the size of the light-harvesting antenna associated with each reaction center (Fig. 1a). Conversely, other taxa acclimate by increasing the number of cellular reaction centers while the antenna size remains relatively constant (Fig. 1b) (Falkowski and Owens 1980; Perry et al. 1981; Dubinsky et al. 1986). These acclimation responses represent two different adaptive traits (Falkowski and Owens 1980). The amount of accessory pigment within the antenna, the amount of chlorophyll per reaction center, and the maximum capacity for carbon fixation can also vary between taxa (Falkowski and Raven 1997).

Shelf seas, with strong horizontal gradients in the degree of water column mixing, are characterized by dynamic ecosystems (e.g., Moore et al. 2003). In stratified waters, the thermocline represents a barrier to transport between high-light surface waters and the low-light subsurface chlorophyll maximum (SCM) (Sharples et al. 2001). Conversely, mixed water columns are characterized by rapid movement of phytoplankton between high and low light (Moore et al. 2003). To understand the interactions of physical forcing and biological response in these systems, observations of phytoplankton physiology need to be made at high vertical, horizontal, and temporal resolution. This requirement has led to the growing use of in situ active fluorescence techniques such as fast repetition rate (FRR) fluorometry for assessment of physiological state and estimation of photosynthetic electron transport rates (Kolber et al. 1990; Suggett et al. 2001; Moore et al. 2003). The FRR technique is capable of measuring a number of parameters that relate to photoacclimation and adaptation, including the functional absorption cross-section of photosystem II (PSII) and the turnover time of the primary PSII electron acceptor (Q_a) (Kolber et al. 1998).

The functional absorption cross-section (σ_{PSII}) is the product of absorption by the suite of PSII antenna pigments and the probability that an exciton within the antenna will cause a photochemical reaction (Mauzerall and Greenbaum 1989). The amount of pigment associated with each PSII reaction center (RCII) will therefore govern much of the variability in σ_{PSII} (Kolber et al. 1988; Suggett et al. 2004). Taxon-dependent differences in antenna accessory pigment, or acclimation responses that alter the ratio of pigment : RCII, thus result in variability of σ_{PSII} within natural populations (Fig. 1a).

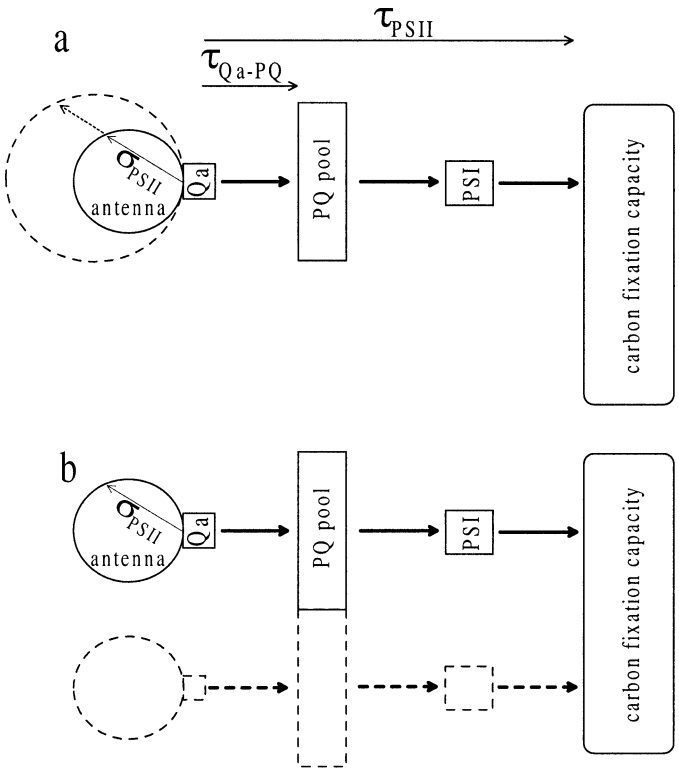

Fig. 1. Simplified schematics of photosynthetic apparatus as related to two contrasting ''strategies'' of photoacclimation. (a) Acclimation to lower irradiance occurs via increases in the ''size'' of the PSII antenna, increasing the functional absorption cross-section of PSII (σ_{PSII}) at constant photosynthetic unit number per unit carbon fixation capacity. The amount of PSII antenna pigment transferring energy to active reaction centers largely governs σ_{PSII}. Hence taxa with higher amounts of chlorophyll or accessory pigment per RCII will also tend to have an adaptively higher σ_{PSII} (Suggett et al. 2004). (b) Acclimation to decreased irradiance occurs by increasing the number of PSIIs of constant cross-section for a given carbon fixation capacity, leaving σ_{PSII} unchanged while decreasing the maximum rate of whole-chain electron transport ($1/\tau_{PSII}$). For simplicity it is assumed that the ratio of PSII : PQ : PSI remains constant during the acclimation process as observed in *Dunaliella tertiolecta* (Sukenik et al. 1987). The relation between $1/\tau_{Q_a-PQ}$ and $1/\tau_{PSII}$ will depend on the extent to which downstream processes limit the reoxidation of Q_a (Kolber and Falkowski 1993).

The rate of Q_a reoxidation ($1/\tau_{Q_a}$) should set an upper limit on the rate of whole-chain electron transport ($1/\tau_{PSII}$). Irradiance-dependent changes in the ratio of RCIIs to carbon fixation capacity (or per cell) appear to control $1/\tau_{PSII}$ during photoacclimation (Sukenik et al. 1987) (Fig. 1b). A change in the number of reaction centers, rather than in the size of the antenna, can potentially alter $1/\tau_{Q_a}$. However, such a response will depend on the degree of downstream control of Q_a reoxidation (Cleland 1998), the extent of cyclic electron flow (Prasil et al. 1996), and differing pathways of reductant use (Behrenfeld et al. 2004). Parameters measured using FRR fluorescence can thus potentially differentiate between the two structural forms of photoacclimation, as well as other adaptive traits.

At high irradiances, damage to RCII can occur, potentially

leading to a reduction in photosynthetic rate (photoinhbition) (Prasil et al. 1992; Long et al. 1994). The probability of RCII damage can be modulated by both σ_{PSII} and the redox state of Q_a (Park et al. 1997; Baroli and Melis 1998). The latter effect likely results from a decreased probability for stabilization of the primary charge separation when Q_a is reduced (Park et al. 1997). The redox state of Q_a will, in turn, be governed by the rates of both light absorption and forward electron transport (Fig. 1).

Under excess irradiance a number of nonphotochemical quenching (NPQ) processes act to dissipate excitation energy and hence protect RCII from damage (Krause and Weis 1991; Horton et al. 1996). In particular, rapidly reversible energy-dependent quenching (q_E), frequently associated with the cycling of xanthophyll pigments in the PSII antenna, can reduce the functional absorption cross-section under ambient irradiance (σ'_{PSII}) (Krause and Weis 1991; Olaizola 1994; Falkowski and Raven 1997). Additionally, quenching associated with photoinhibition (q_I), which relaxes over much longer timescales than q_E, may be significant (Morrison 2003); however, the site and mechanism of q_I remains equivocal (Krause and Weis 1991; Horton et al. 1996). Photoacclimation, photoprotection, and photodamage/inhibition are thus coupled processes requiring joint consideration (Behrenfeld et al. 1998).

Recent models of photoacclimation suggest that the alteration of cellular pigment is a mechanism for balancing the energy captured by light absorption with the energy demand for growth (Geider et al. 1998). These models are conceptually consistent with the redox state of the plastoquinone (PQ) pool providing the controlling signal for photoacclimation (Escoubas et al. 1995). However, there are limits on the extent to which a given taxon can modulate pigment content relative to carbon fixation capacity (MacIntyre et al. 2002), and thus on its ability to compete in a given light environment. Presumably, the taxonomic composition of the phytoplankton responds to different environments through selection of genotypes that are better adapted to the prevailing light and nutrient environment (Richardson et al. 1983; Cullen and MacIntyre, 1998). Therefore, interpretation of natural variability in phytoplankton photosynthetic performance requires an understanding of the relative importance of acclimation and adaptation in an ecological setting.

In the current study, we investigated photoacclimation and photoadaptation of natural populations in a shelf sea region during summer. We provide the first demonstration that, within the natural system studied, marked vertical gradients in acclimation state primarily result from changes in the number of PSII reaction centers per cell. In contrast, observed spatial (horizontal) variability in the PSII antenna size was primarily driven by changes in accessory pigmentation related to taxonomic gradients. These results are discussed in the context of current physiological models, the balance of electron transport and carbon fixation, and the ecological setting of the natural populations.

Methods

General—Data were collected in July–August 2003 during a cruise of the RRS *James Clark Ross* (JR98). Sites were occupied in the stratified region of the Celtic Sea shelf and shelf break and at a mixed site within the Irish Sea (Fig. 2). Incident surface solar irradiance integrated from 400 to 700 nm, hereafter referred to as photosynthetically available radiation (PAR), was recorded continuously. Hydrographic data at each site were collected using a SeaBird 911 conductivity, temperature, depth (CTD) interfaced with a Chelsea Instruments Aquatracka MKIII in situ chlorophyll fluorometer. Two Chelsea Instruments Fastracka FRR fluorometers, each interfaced with a 2π PAR sensor, were also deployed in situ on the CTD frame. Optical depths (OD) were calculated from vertical PAR profiles. In situ irradiance at seven discrete wavelengths was also measured using a Licor Li-1800 UW spectroradiometer.

Water was sampled using 10-liter Niskin bottles. Four of the sites, CS1, CS2, CS3, and IS1 (Fig. 2), were occupied for 24-h periods on 31 July, 29 July, 05 August, and 02 August respectively. This enabled the collection of multiple samples of both surface and deeper phytoplankton populations throughout the photoperiod. Additionally the CS1 and CS3 sites were resampled on 10 and 11 August respectively. Four additional sites were only sampled with a single CTD cast, typically at two depths (Fig. 2).

Phytoplankton community structure—Taxonomic variability was assessed using a combination of high-performance liquid chromatography (HPLC) (see following), size-fractionated chlorophyll, flow cytometry, and microscopic identification and enumeration of preserved samples. Flow cytometry data were used to estimate the contribution of small eukaryotes and cyanobacteria (*Synechococcus*) to total autotrophic community biovolume and the cellular fluorescence to biovolume ratio (F : cell vol). Only relative changes in biovolume are reported.

FRR fluorometry measurements and analysis—To eliminate the influence of short-term kinetic responses, including nonphotochemical quenching and state transitions, active fluorescence measurements were principally performed on discrete samples. Samples were left in the dark for >30 min in a temperature-controlled environment before measurement. This protocol allowed relaxation of q_E (data not shown); however, some long-lived q_I may have remained (Krause and Weis 1991; Horton et al. 1996). The FRR fluorometer was programmed to deliver sequences of 100 1.1-μs saturation flashes at 2.8-μs intervals followed by 20 1.1-μs relaxation flashes at 98.8-μs intervals. Nonlinearity in instrument response was characterized using extracts of chlorophyll *a* (Chl *a*) (Laney 2003). Blanks were run on filtrates from each sample (Cullen and Davis 2003). Correction for the contribution of the blank had no significant influence on values of σ_{PSII} or $1/\tau_{Q_a}$, these parameters being dependent on rates of change of fluorescence and thus relatively insensitive to the baseline.

Induction curves were averaged over 160 individual sequences to minimize error (Suggett et al. 2004). The fluorescence transient (f) at time t was then fitted to the following biophysical model (Kolber et al. 1998):

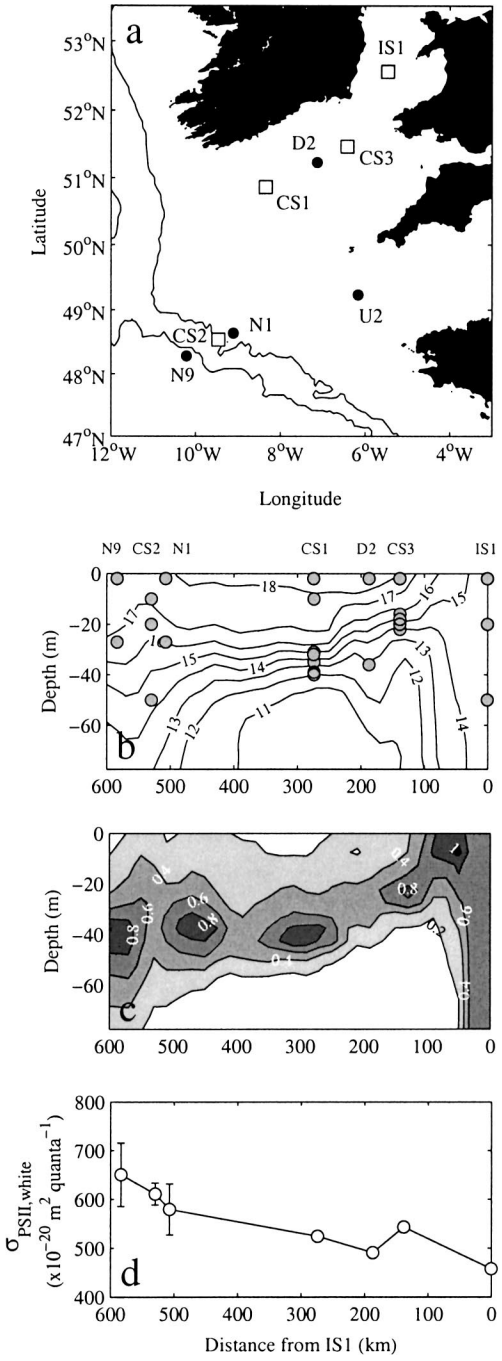

Fig. 2. (a) Map of study area and stations. Solid lines indicate 200 m and 2,000 m depth contours. Open squares indicate positions of the four principal sampling stations. (b) Temperature section through study region along a line from IS1-CS3-D2-CS1-N1-CS2-N9. Symbols indicate sampling depths and locations for physiological measurements. (c) Fluorescence section through study region. Fluorescence values are scaled to approximate the chlorophyll concentration; however, the fluorescence yield varied both vertically and horizontally throughout. (d) Water column mean $\sigma_{\mathrm{PSII,white}}$ versus cross-shelf distance from IS1. Error bars are 1 SE.

$$f(t) = F_0 + (F_m - F_0)\left[C(t)\frac{1-p}{1-C(t)p}\right] \quad (1)$$

where p is a connectivity parameter and F_0 and F_m are the minimum and maximum fluorescence yields respectively. The fraction of closed (reduced) reaction centers ($C(t)$) was determined iteratively using:

$$\frac{\mathrm{d}C(t)}{\mathrm{d}t} = i(t)\sigma_{\mathrm{PSII}}\frac{1-C(t)}{1-C(t)p} - \frac{C(t)}{\tau_{Q_a}} \quad (2)$$

where $i(t)$ is the flash intensity (Kolber et al. 1998). Equations 1 and 2 were used to define both saturation and relaxation components of the fluorescence induction curve simultaneously with revised software run in MATLAB™ based on original codes provided by S. Laney (Laney 2003). The revised software used the asymptotic value reached during the relaxation part of the curve, given by the steady-state solution of Eq. 2 (see Kolber et al. 1998 their Eq. 15), to improve estimation of τ_{Q_a}. Because of the constant delay between relaxation flashes for the commercial instrument used in this study, only one component of the rate of Q_a reoxidation could be measured (Kolber et al. 1998). The relaxation protocol was 2 ms in duration, allowing an estimate of $1/\tau_{Q_a}$ for the mean value of transport from Q_a through the PQ pool (Crofts et al. 1993; Falkowski and Raven 1997). Hereafter the term $1/\tau_{Q_a \rightarrow \mathrm{PQ}}$ is used to represent the estimate of electron transport rate directly obtained by FRR fluorometry.

Estimates of RCII abundance—To obtain a sample of sufficient density for measurements of RCII abundance, natural phytoplankton populations were concentrated under a gentle vacuum onto 47-mm diameter, 0.2-μm pore size polycarbonate filters. Material collected onto the filters was resuspended in 4–5 mL of filtrate. The maximum PSII photochemical efficiency (F_v/F_m) was measured using the FRR fluorometer before and after concentration. Samples with a significantly lower F_v/F_m following concentration were discarded. Oxygen flash yields were measured according to Suggett et al. (2004) using a Hansatech Instruments Clarke-type electrode housed within a DW1 liquid-phase oxygen electrode chamber and a single turnover saturation flash system. The time-consuming concentration step provided few measurable suspensions from low chlorophyll surface water samples. Resolution of depth variability in RCII abundance was therefore not possible. The ratio of Chl *a* to PSII reaction centers is reported throughout as the product of Chl *a* $(O_2)^{-1}$ and 0.25 mol O_2 (mol RCII)$^{-1}$ giving mol Chl : mol RCII.

Spectral absorption, fluorescence, and pigments—Spectral absorption was routinely measured on board using samples filtered through 25-mm Whatman GF/F filters following the method of Tassan and Ferrari (1995) on a Hitachi U-3000 spectrophotometer fitted with a ϕ60 integrating sphere. Spectra were measured before and after depigmentation using 1–2% NaClO. Concentrated suspensions were used to derive wavelength-dependent path-length amplification factors (β) for each site. Absorption was normalized to Chl *a*

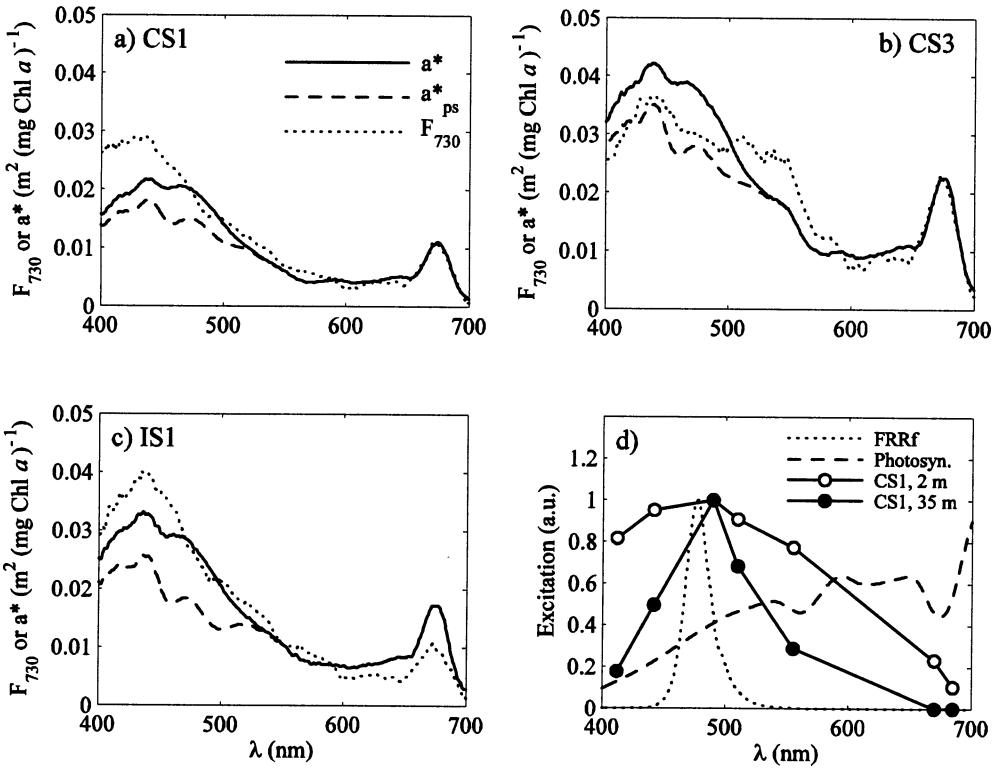

Fig. 3. (a–c) Spectral dependence of 730-nm fluorescence excitation, chlorophyll-specific optical absorption (a^*) and a^* corrected for absorption by nonphotosynthetic pigments (a^*_{ps}) from stations CS1 (a), CS3 (b), and IS1 (c). (d) Normalized FRR fluorometer and photosynthetron excitation spectra compared with in situ spectra at depths of 2 m and 35 m at CS1.

to derive the chlorophyll-specific absorption spectra (a*(λ)). Fluorescence excitation spectra at 730 nm (F_{730}) were also measured using a Perkin Elmer LS50B on the same suspension as that used for RCII abundance, using methods described previously (Suggett et al. 2004).

HPLC samples were filtered through 25-mm Whatman GF/F filters and stored at −80°C. On return to the laboratory, pigments were extracted into 90% acetone using sonication. Extracts were analyzed according to the method of Barlow et al. (1993) on a Thermo Separation products HPLC. Pigments were identified by retention time and on-line diode array spectroscopy. Absorption by total pigments ($a^*_{pig}(\lambda)$) including chlorophylls *a*, *b*, and *c*; photosynthetic carotenoids (PC); and nonphotosynthetic carotenoids (NPC) was reconstructed using the method of Bidigare et al. (1990) as described in Suggett et al. (2004). Absorption by photosynthetic pigments ($a^*_{pspig}(\lambda)$) was reconstructed in a similar manner excluding the contribution of NPCs. Optical absorption ($a^*(\lambda)$) was weighted by the ratio of $a^*_{pspig}(\lambda)/a^*_{pig}(\lambda)$ to obtain a measure of the optical absorption by photosynthetic pigments ($a^*_{ps}(\lambda)$) (Fig. 3).

The physiological or ecological relevance of spectrally dependent parameters (e.g., σ_{PSII}) needs to be assessed with reference to the relevant excitation spectra (Suggett et al. 2001, 2004). Thus, for example, assessment of variability in σ_{PSII} by weighting to a spectrally flat (white) light source gives a less arbitrary measure of the absorption cross-section than the instrument-specific value measured at any given wavelength (Fig. 3d). Further, assessment of ecological relevance requires weighting to the spectral distribution of light in situ. Hereafter, as necessary, we report all spectrally dependent parameters with a subscript denoting the relevant excitation wavelength(s). Thus to derive a value of optical absorption directly comparable to the FRR fluorometry measurement of σ_{PSII} at 478 nm ($\sigma_{PSII,478}$), $a^*_{ps}(\lambda)$ was weighted by the excitation spectrum of the FRR fluorometer to derive $a^*_{ps,478}$ (Fig. 3) (Suggett et al. 2004):

$$a^*_{ps,478} = \frac{\sum_{400–700\ nm} a^*_{ps}(\lambda)E_{FRR}(\lambda)}{\sum_{400–700\ nm} E_{FRR}(\lambda)} \quad (3)$$

Similarly, values of σ_{PSII} weighted to a spectrally flat (white) light source ($\sigma_{PSII,white}$) and estimates of σ_{PSII} weighted to the spectral light distribution in situ $\sigma_{PSII,in\ situ}$ were calculated using:

$$\sigma_{PSII,white} = \sigma_{PSII,478}\frac{\sum_{400–700\ nm} a^*(\lambda) \sum_{400–700\ nm} E_{FRR}(\lambda)}{300 \sum_{400–700\ nm} a^*(\lambda)E_{FRR}(\lambda)} \quad \text{and}$$

$$\sigma_{PSII,in\ situ} = \sigma_{PSII,478}\frac{\sum_{400–700\ nm} a^*(\lambda)E_{in\ situ}(\lambda) \sum_{400–700\ nm} E_{FRR}(\lambda)}{\sum_{400–700\ nm} a^*(\lambda)E_{FRR}(\lambda) \sum_{400–700\ nm} E_{in\ situ}(\lambda)} \quad (4)$$

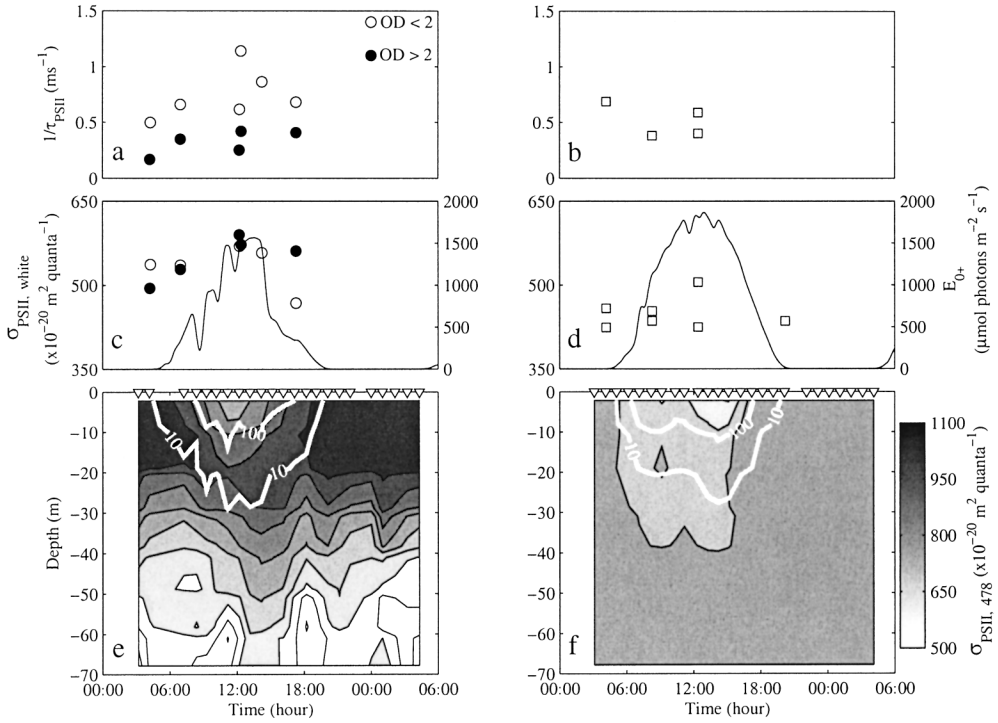

Fig. 4. Diel variability in physiological parameters at stratified CS3 (a, c, and e) and vertically mixed IS1 (b, d, and f). (a–b) Rate of whole-chain electron transfer ($1/\tau_{PSII}$) calculated using Eq. 6. (c–d) $\sigma_{PSII,white}$ and incident surface irradiance. (e–f) $\sigma'_{PSII,478}$ measured in situ using profiling FRR fluorometer with 100 and 10 μmol m^2 s^{-1} photons isolumes superimposed. Symbols indicate times of vertical FRR fluorometer and PAR profiles. Data in (a) and (c) correspond to two occupations of CS3 on 05 August and 11 August; data in (e) correspond to the 05 August occupation. The SCM at CS3 was at a depth of 20 m.

where $E_{FRR}(\lambda)$ and $E_{in\ situ}(\lambda)$ refer to the excitation spectra of the FRR fluorometer and in situ irradiance field respectively. In situ spectral irradiance data were only available from stations CS1, CS3, and IS1. We thus used spectra measured at CS1 to approximate $E_{in\ situ}(\lambda)$ at the other open shelf sites (Fig. 3d). The calculated spectrally dependent values of the functional absorption cross-section ($\sigma_{PSII,478}$, $\sigma_{PSII,white}$, and $\sigma_{PSII,in\ situ}$) all remained highly correlated ($R^2 > 0.85$, $n = 35$) despite the differing excitation wavelengths. However, absolute values varied with $\sigma_{PSII,white}$ a factor of 0.6 (range 0.56–0.70) lower than $\sigma_{PSII,478}$. Additionally, the FRR fluorometer excitation spectrum more closely approximates the in situ spectrum at depth (Fig. 3d). Differences between $\sigma_{PSII,in\ situ}$ and $\sigma_{PSII,478}$ were thus depth dependent, with $\sigma_{PSII,in\ situ}$ 0.69 and 0.83 lower than $\sigma_{PSII,478}$ in the surface and at the SCM respectively.

^{14}C P versus E curves—The irradiance dependence of photosynthetic carbon fixation was measured at in situ temperature using short-term (2–4 h) *P* versus *E* incubations in a photosynthetron. Data from *P* versus *E* experiments, normalized to the Chl *a* concentration, were used to calculate the maximal chlorophyll-specific photosynthetic carbon fixation rate (P^*_{max}), the maximum light utilization coefficient (α^*), and the light-saturation parameter ($E_k = P^*_{max}/\alpha^*$). In a similar manner to $\sigma_{PSII,(\lambda)}$, values of E_k were scaled to account for spectral differences between the photosynthetron and both in situ ($E_{k,in\ situ}$) and FRR fluorometer spectra ($E_{k,478}$) using:

$$E_{k,478} = E_{k,phot}\frac{\sum_{400-700\ nm} a^*(\lambda)E_{phot}(\lambda)\ \sum_{400-700\ nm} E_{FRR}(\lambda)}{\sum_{400-700\ nm} a^*(\lambda)E_{FRR}(\lambda)\ \sum_{400-700\ nm} E_{phot}(\lambda)} \quad \text{and}$$

$$E_{k,in\ situ} = E_{k,phot}\frac{\sum_{400-700\ nm} a^*(\lambda)E_{phot}(\lambda)\ \sum_{400-700\ nm} E_{in\ situ}(\lambda)}{\sum_{400-700\ nm} a^*(\lambda)E_{in\ situ}(\lambda)\ \sum_{400-700\ nm} E_{phot}(\lambda)} \quad (5)$$

where the subscript ''phot'' indicates a quantity measured or weighted by the spectral irradiance within the photosynthetron (Fig. 3d). Values of $E_{k,478}$ and $E_{k,in\ situ}$ were factors of 0.47 (range 0.41–0.60) and 0.63 (range 0.58–0.73) lower than measured values of $E_{k,phot}$ respectively. Corrections performed using absorption spectra with the contribution of NPCs removed were around 20% higher.

The rate of whole-chain electron transport from charge separation to carbon fixation ($1/\tau_{PSII}$) was calculated from the product of the ^{14}C estimates of $E_{k,478}$ and the FRR fluorometry estimates of $\sigma_{PSII,478}$ (Falkowski and Raven 1997; Behrenfeld et al. 1998), i.e.:

$$1/\tau_{PSII} = E_{k,478}\sigma_{PSII,478} \quad (6)$$

Results

Hydrographic setting and taxonomy—Hydrographic conditions were typical of summer in the study region (Fig. 2b). Strong thermal stratification was observed throughout most of the Celtic Sea, with weaker stratification at the shelf edge and fully mixed conditions due to strong tides in the Irish Sea. An SCM was observed at all the stratified sites (Fig. 2c, Table 1). The peak of the SCM was typically situated at a depth corresponding to around 5% of surface irradiance. As previously observed (Sharples et al. 2001), considerable patchiness in SCM chlorophyll concentration was apparent (Fig. 2c).

Phytoplankton cells <5 μm in diameter dominated throughout most of the region (Table 1). Flow cytometry data indicated that small eukaryotes dominated total community biovolume at all stations apart from CS3 where *Synechococcus* numbers reached $>100 \times 10^6$ L^{-1} in and above the SCM, contributing 50–80% of the total autotrophic biovolume. The importance of the cyanobacteria was apparent in fluorescence and absorption spectra obtained at CS3 that displayed peaks or shoulders from 500 to 550 nm due to the presence of phycobiliproteins (Fig. 3b). Marker pigment ratios suggested that flagellates belonging to the prymnesiophytes and pelagophytes comprised much of the eukaryotic population, the latter group becoming more important toward the shelf edge (Table 1). Light microscopy indicated that the higher fucoxanthin : Chl *a* ratio observed at CS2 resulted from the presence of pennate diatoms. Estimates of autotrophic biovolume from flow cytometry data (Table 1) excluded the (typically minor) contribution of such larger eukaryotes. Acknowledging this limitation, ratios of total community biovolume to total chlorophyll were generally higher in the surface than within the SCM (Table 1).

PSII antenna characteristics—Physiological parameters relating to the makeup of the PSII antenna for the four main sites are presented in Table 2. Estimates of the Chl *a* : RCII ratio for natural populations were within the range reported for cultures (e.g., Dubinsky et al. 1986; Suggett et al. 2004). Values at eukaryote-dominated sites were around 630–720 mol mol^{-1} (Table 2). Prokaryotes typically have lower Chl *a* : RCII ratios (Kolber and Falkowski 1993; Suggett et al. 2004) and a significantly lower value of 530 mol mol^{-1} was observed for the *Synechococcus*-dominated community at CS3 (Tables 1 and 2).

The PC : Chl *a* ratio varied markedly between stations, with a general decrease from the shelf edge through the stratified waters to the mixed station (Tables 1 and 2). Intersite differences in PC : Chl *a* were accompanied by variability in accessory pigment composition and were thus ascribed to taxonomic differences (Table 1). Vertical differences in PC : Chl *a* were only significant at CS2. Both surface and deeper populations were collected from a deeper optical depth (lower within the photic zone) at CS2. Deeper populations were sampled below the SCM and 1% light level at this station, complicating direct comparison of vertical physiological variability with the other stratified sites.

In contrast to the PC : Chl *a* ratios, NPC : Chl *a* varied little between sites. A significant increase in NPC was observed in the surface at strongly stratified sites as would be expected given a photoprotectant role for these pigments (Table 2). Intersite variability in PC : Chl *a* and Chl *a* : RCII resulted in a decrease in PC : RCII from the shelf edge toward the mixed water. The optical absorption cross-section (a^*_{478}) did not vary significantly between sites but increased toward the surface in stratified waters.

Measured values of $\sigma_{PSII,478}$ were significantly higher at the shelf edge than on shelf, with lowest values at the mixed site (Table 2). Calculated values of $\sigma_{PSII,white}$ displayed a similar pattern (Fig. 2d). The functional absorption cross-section was typically invariant with depth within and above the SCM (Table 2). Decreases in $\sigma_{PSII,478}$ frequently occurred below the SCM at stratified sites (Fig. 4e). Diel variability in $\sigma_{PSII,478}$ or $\sigma_{PSII,white}$ was limited. A minor (10%) increase in $\sigma_{PSII,white}$ was observed in the surface at midday at CS3 (Fig. 4c,d). In contrast, decreases in $\sigma'_{PSII,478}$ measured in situ indicated the presence of significant antenna-based NPQ within surface populations, particularly at stratified stations (Fig. 4e,f).

Much of the variability in the functional absorption cross-section throughout the study region could be explained by changes in accessory pigmentation. In particular, the ratio of 19′-butanoyloxyfucoxanthin to Chl *a* was highly positively correlated to $\sigma_{PSII,478}$ (Fig. 5a), as was the ratio of 19′-hexanoyloxyfucoxanthin to Chl *a* ($r^2 = 0.452$, $n = 31$, $p < 0.001$) (not shown). Similar relations were found for $\sigma_{PSII,white}$. Measured PSII cross-sections thus largely reflected the relative dominance of different types of flagellate populations. The ratio PC : Chl *a* explained 45% of the variance in $\sigma_{PSII,478}$ and 50% of the variability in $\sigma_{PSII,white}$ ($p < 0.001$). For a reduced data set ($n = 13$) where Chl *a* : RCII estimates were available, the PC : RCII and PC : Chl *a* ratios could each explain around 60% of the variance in $\sigma_{PSII,478}$ or $\sigma_{PSII,white}$ (not shown). As previously noted (Moore et al. 2005), such covariability is expected at 478 nm, i.e., overlapping the absorption band of the photosynthetically active carotenoids. The similarity of the relations when considering $\sigma_{PSII,white}$ likely reflected the large proportion of the total cellular absorption that could be attributed to the PCs for the sampled populations (Table 2).

Using the spectral fluorescence, absorption, and Chl *a* : RCII data, an independent estimate of $\sigma_{PSII,478\,calc}$ can be derived from (Suggett et al. 2004):

$$\sigma_{PSII,478calc} = \frac{a^*_{ps,478} 0.5 F_{730} : a^*}{RCII : Chl a} \quad (7)$$

where 0.5 $F_{730} : a^*$ is assumed to indicate the proportion of absorbed light that is transferred to PSII, estimated by scaling the measured fluorescence excitation spectrum to the absorption spectrum (see Suggett et al. 2004 and references therein).

The ratio $F_{730} : a^*$ dropped from around 1 at CS1, CS2, and IS1 to 0.8 at CS3. Hence half the absorbed energy at 478 nm was transferred to PSII at the eukaryote-dominated stations (Table 2), with significantly less (40%) transferred to PSII at the *Synechococcus*-dominated CS3 station, again consistent with laboratory data (Suggett et al. 2004). For populations ($n = 13$) where spectral fluorescence and esti-

Table 1. Taxonomic and pigment data collected in Celtic and Irish Seas during summer 2003. Sites are ordered from left (shelf edge) to right (mixed water) (Fig. 2). Mean values (±1 SE, where $n > 1$) of surface and SCM chlorophyll and total autotrophic community biovolume (Bvol) are presented for each site. Biovolume estimates exclude the contribution of large eukaryotes. Size fractionated chlorophyll, cell numbers (Syn, *Synechococcus*, Euk, eukaryotes) and marker pigment to chlorophyll *a* ratios are presented as water column means (±1 SE). Vertical taxonomic variability was minor; sampling depths are indicated in Fig. 2b. Marker pigments and likely group: 19′-butanoyloxyfucoxanthin (But, Pelagophytes), 19′-hexanoyloxyfucoxanthin (Hex, Prymnesiophytes), fucoxanthin (Fuco, Diatoms); together these three pigments comprised >80% of the photosynthetic carotenoid present in all the samples.

	N9	CS2	N1	U2	CS1	D2	CS3	IS1
Chl (surf) (μg L^{-1})	0.43	0.25±0.01	0.34	0.17	0.29±0.07	0.37	0.49±0.04	0.57±0.04
Chl (SCM) (μg L^{-1})	0.57	0.39±0.04	0.95	0.38	1.01±0.27	0.53	1.06±0.14	SCM absent
Bvol (surf) (rel.)	0.72	0.66±0.08	0.54	0.73	0.60±0.08	n.d.*	1.41±0.06	0.42±0.02
Bvol (SCM) (rel.)	0.86	1.00±0.54	0.69	0.19	0.85±0.10	0.73	1.26±0.3	SCM absent
% Chl <5μm	n.d.	46±7	59±4	61±10	77±3	n.d.	81±4	66±4
Syn ($\times 10^6$ L^{-1})	34±13	21±11	38±4	13±10	35±4	38	105±14	6.3±0.7
Euk ($\times 10^6$ L^{-1})	8.0±3	8.4±2	3.0±1.3	5.4±3	7.8±0.5	2	12±1	5.6±0.7
But:Chl (g:g)	0.18±0.05	0.18±0.03	0.10±0.01	0.05±0.01	0.09±0.004	0.05±0.002	0.08±0.003	0.02±0.002
Hex:Chl (g:g)	0.40±0.05	0.34±0.04	0.38±0.05	0.31±0.07	0.36±0.03	0.28±0.01	0.32±0.008	0.12±0.01
Fuco:Chl (g:g)	0.21±0.06	0.40±0.02	0.18±0.02	0.17±0.07	0.23±0.02	0.28±0.10	0.21±0.01	0.28±0.02

* n.d., no data available.

Table 2. Physiological parameters related to antenna structure for principal stations. Values are quoted as mean (±1 SE). Surface samples were taken as being above an optical depth of 2 and deep samples as being below an optical depth of 2. For the majority of stratified sites the 'deep' samples were collected within the subsurface chlorophyll maximum (SCM), the exception being at CS2 where some samples were collected below the SCM (Fig. 2b, c). Mean values of all parameters showed significant differences between sites (ANOVA) excepting a^*_{478}. Letters in italics (*a–d*) indicate site-specific means indistinguishable at 95% confidence level (Tukey–Kramer test). Mean values between surface and SCM compared by *t*-test, marked *, **, or *** where significant ($p < 0.05$, 0.01, 0.001, respectively).

		CS2	CS1	CS3	IS1
Chl *a* : RCII		703±11	717±17	527±7	631±13
(mol : mol)		*a*	*a*	*b*	*c*
PC : Chl *a*	Surface	1.12±0.03	0.74±0.04	0.61±0.017	0.52±0.004
(g : g)	Deep	0.82	0.75±0.03	0.68±0.025	
		a, ***	*b,c*	*b,c,d*	*c,d*
NPC : Chl *a*	Surface	0.18±0.02	0.29±0.02	0.29±0.02	0.24±0.02
(g : g)	Deep	0.17	0.18±0.003	0.21±0.01	
		a	*a,b*, ***	*b*, *	*a,b*
PC : RCII		0.73±0.012	0.50±0.006	0.33±0.002	0.29±0.004
(g μmol^{-1})		*a*	*b*	*c*	*c*
a^*_{478}	Surface	3.6±0.4	4.8±0.8	4.6±0.7	2.8±0.3
($\times 10^{-2}$ m^2	Deep	3	2.2±0.5	3.8±0.1	
[mg Chl *a*]$^{-1}$)			*		
$\sigma_{PSIL,\,478}$	Surface	1083±27	896±14	937±27	729±18
($\times 10^{-20}$ m^2	Deep	912±28	900±11	893±28	
quanta^{-1})		*a*, *	*b*	*b*	*c*
0.5 $F_{730\,:\,a^*}$		0.48±0.01	0.49±0.01	0.40±0.01	0.51±0.01
		a	*a*	*b*	*a*

mates of Chl *a* : RCII were available, measured values of $\sigma_{PSII,478}$ and those estimated using Eq. 7 were well correlated and of comparable magnitude (Fig. 5b). Close correspondence between the two independent estimates provided confidence in ascribing observed gradients in $\sigma_{PSII,478}$ or $\sigma_{PSII,white}$ to changes in the photosynthetic pigment : RCII ratio (Table 2, Fig. 5). The data also provide confidence in the techniques used and extend the results of Suggett et al. (2004) obtained for cultures covering a wide range of taxa to field populations.

Light saturation and electron transport—Rates of Q_a reoxidation estimated by FRR fluorometry were similar for the three main shelf sites and slightly lower at CS2 (Table 3). Differences between sites were minimal in all other photosynthetic parameters related to light saturation or maximum rates of electron transport or carbon fixation; however, a marked depth dependence was observed (Table 3). The parameters, $1/\tau_{Q_a\rightarrow PQ}$, $E_{k,478}$, and P^*_{max}, were higher at the surface (OD < 2) than at depth (OD > 2) for the stratified sites (Fig. 6, Table 3), these differences being significant where

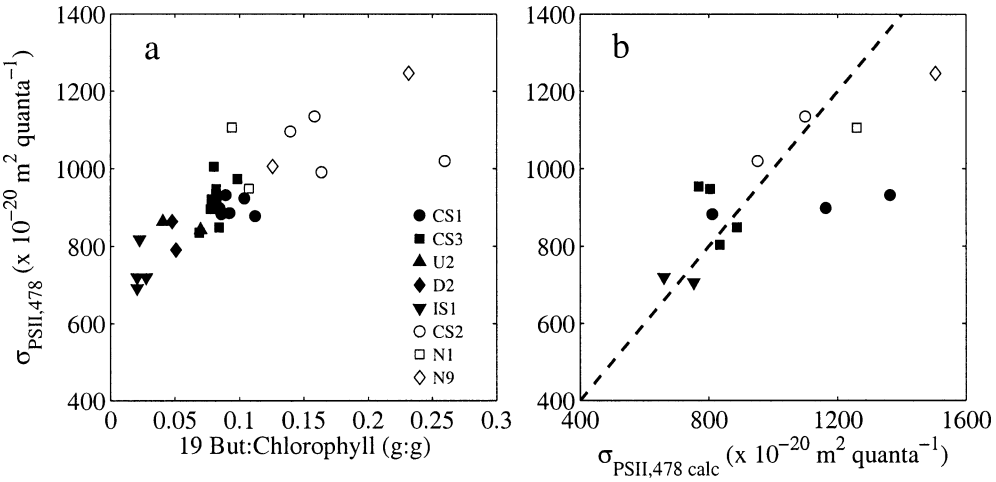

Fig. 5. (a) Relation between σ_{PSII} and the 19′-butanoyloxyfucoxanthin : Chl *a* ratio ($r^2 = 0.636$, $n = 31$, $p < 0.001$). (b) Comparison of σ_{PSII} as directly measured using FRR fluorometry and independently estimated using Eq. 7 ($r^2 = 0.558$, $n = 13$, $p < 0.005$), neglecting the transfer term in Eq. 7 ($F_{730} : a^*$) reduced the variance explained by <2%. Symbols correspond to sites, open symbols indicate sites toward shelf edge. Dotted line in (b) indicates 1 : 1 relation.

Table 3. Parameters related to light saturation and rates of photosynthetic electron transport for principal stations. Surface samples were taken as being above an optical depth of 2 and deep samples as being below an optical depth of 2. There were no significant differences at 95% confidence level between sites excepting lower $1/\tau_{Qa}$ at the shelf edge (ANOVA). The latter may have resulted from deeper optical depths being sampled at this station. Mean values between surface and SCM compared by *t*-test, marked *, **, or *** where significant ($p < 0.05$, 0.01, 0.001, respectively).

		CS2	CS1	CS3	IS1
$1/\tau_{Qa\rightarrow PQ}$ (ms^{-1})	Surface	0.40±0.06	0.66±0.02	0.69±0.04	0.66±0.03
	Deep	0.37±0.06	0.46±0.03	0.56±0.03	
			***	**	
$E_{k,478}$ (μmol photons m^{-2} s^{-1})	Surface	74±5	101±2	128±13	117±14
	Deep	37	45±4	58±8	
			***	**	
P^*_{max} (mol C [g Chl *a*]$^{-1}$ h^{-1})	Surface	0.35±0.03	0.28±0.03	0.44±0.05	0.45±0.08
	Deep	0.21	0.18±0.02	0.21±0.02	
			*	**	

sufficient data were available to perform statistical tests (Table 3). Variability in P^*_{max} was dominated by changes of similar magnitude in $E_{k,478}$ ($r^2 = 0.666$, $n = 35$, $p < 0.001$, not shown), with mean surface values being more than double those of deep (SCM) samples. In contrast, no correlation was observed between P^*_{max} and α^*_{phot}. Hence changes in *P* versus *E* parameters within the system studied were dominated by "E_k-dependent" variability with minimal "E_k-independent" variability (Behrenfeld et al. 2004).

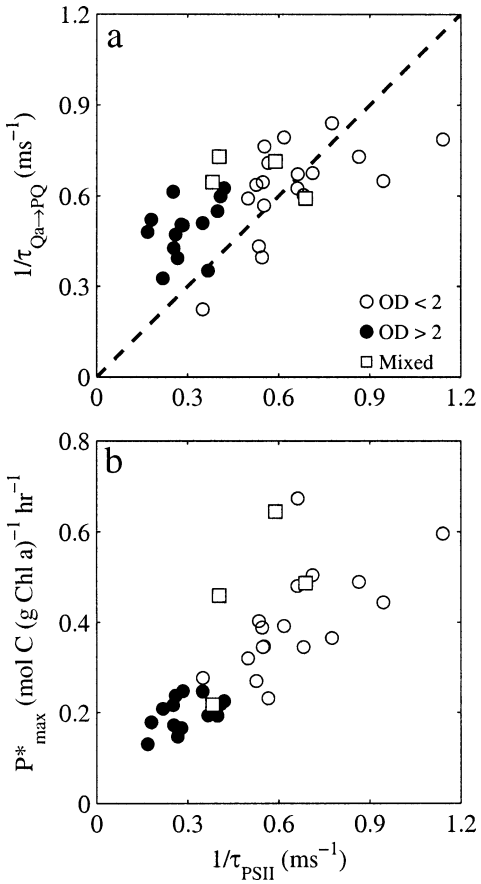

Fig. 6. Relations of rate of whole-chain electron transport ($1/\tau_{PSII}$) as calculated using Eq. 6 to (a) $1/\tau_{Q_a\rightarrow PQ}$ measured by FRR fluorometry ($r^2 = 0.425$, $n = 35$, $p < 0.001$) and (b) P^*_{max} measured by ^{14}C *P* versus *E* incubation ($r^2 = 0.624$, $n = 35$, $p < 0.001$). Squares indicate the mixed station (IS1); circles, stratified stations; open, OD < 2; filled, OD > 2. Dotted line in (a) indicates 1:1 relation.

Measured values of $1/\tau_{Q_a\rightarrow PQ}$ using FRR fluorometry were significantly correlated with independent estimates of $1/\tau_{PSII}$ calculated using Eq. 6 for the complete data set (Fig. 6a). Rearrangement of Eq. 6 and substitution of $\tau_{Q_a\rightarrow PQ}$ for τ_{PSII} also allowed calculation of the light saturation intensity of electron transport ($E_{k\,ETR,478}$) purely from FRR fluorometry-derived parameters. A significant correlation between $E_{k\,ETR,478}$ and the ^{14}C-derived estimates of $E_{k,478}$ was also found ($r^2 = 0.416$, $n = 35$, $p < 0.001$, not shown). To our knowledge, these data represent the first reported comparison of $1/\tau_{Q_a\rightarrow PQ}$ measured using FRR fluorometry with other independently derived and related physiological parameters for natural communities.

The maximum chlorophyll-specific rate of carbon fixation should be related to the rate of whole-chain electron transport and the Chl *a*:RCII ratio according to (Falkowski and Raven 1997):

$$P^*_{max} = \frac{\text{RCII}:\text{Chl}a}{\tau_{PSII}} \tag{8}$$

Vertical gradients in $1/\tau_{PSII}$ accounted for >60% of the variance in P^*_{max} (Fig. 6b). Although this relation contained a degree of circularity, as derivation of $1/\tau_{PSII}$ depends on measurement of E_k and hence P^*_{max} (cf. Eqs. 6 and 8), it is consistent with our observation of a low (1.5-fold) range of variation in Chl *a*:RCII (Table 2) and indicates that changes in maximal electron transport rates are the main cause of the >fourfold range in P^*_{max}. Similarly, vertical gradients in $1/\tau_{Q_a\rightarrow PQ}$ explained a significant proportion of the variance in P^*_{max} ($r^2 = 0.296$, $n = 35$, $p < 0.001$).

Diel variability in photosynthetic parameters related to maximum rates of electron transport or carbon fixation was apparent from the limited time series data for surface populations at CS3 (Fig. 4a). In particular $1/\tau_{PSII}$ was approximately double the predawn value at midday on the 10th of August.

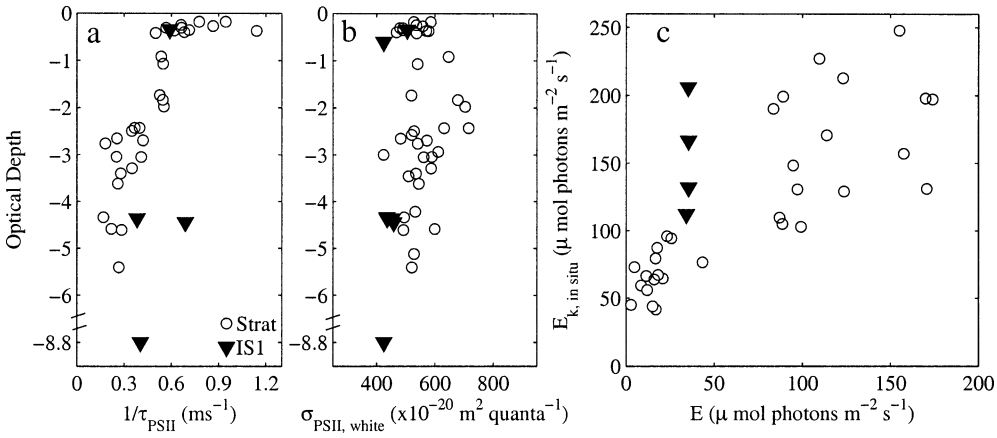

Fig. 7. Relation of photosynthetic parameters to optical depth (OD) and estimated mean 24-h irradiance. (a) $1/\tau_{PSII}$ versus OD (significant correlation observed for stratified sites, $r^2 = 0.725$ (0.761 for log-transformed $1/\tau_{PSII}$), $n = 31$, $p < 0.001$). (b) σ_{PSII} versus OD, no significant relation found. (c) $E_{k,\text{in situ}}$ from ^{14}C P versus E data as a function of estimated mean daily irradiance. (For stratified stations, $r^2 = 0.702$, $n = 31$, $p < 0.001$).

Relation of E_k *to irradiance*—A highly significant correlation of $E_{k,478}$ with OD was found for the subset of data collected at stratified stations ($r^2 = 0.749$ [0.780 for log-transformed $E_{k,478}$], $n = 31$, $p < 0.001$, not shown). The lack of vertical variability in $\sigma_{PSII,478}$ or $\sigma_{PSII,white}$ (Table 2, Fig. 4e) indicates that changes in $E_{k,478}$ were dominated by changes in $1/\tau_{PSII}$ (Eq. 6) (Fig. 7). Additionally, over 50% of the variance in $E_{k,478}$ could be explained by differences in $1/\tau_{Q_a \rightarrow PQ}$.

The mean irradiance experienced for each population was estimated by modeling the light history over the previous 24 h using surface PAR and the OD corresponding to the sampling depth. For samples within the surface mixed layer or at IS1, it was assumed that turbulent mixing cycled cells through the layer on timescales short enough that the mean irradiance within the layer was representative. Confidence in such an approximation at IS1 is provided by previous estimates of mixing timescales at other similar sites (Moore et al. 2003). The potential peak daily irradiance experienced was estimated in a similar manner.

Calculated $E_{k,\text{in situ}}$ strongly correlated with estimated mean daily irradiance for the stratified stations (Fig. 7c). At the mixed station (IS1) no vertical gradient was observed in any of the physiological parameters, implying that the mixing timescale was shorter than the photoacclimation timescale (Lewis et al. 1984; Moore et al. 2003). The mean irradiance calculated for the mixed station (35 μmol photons m^2 s^{-1}) was 7–8% of surface values, equivalent to that for the SCM at stratified stations (Fig. 7a). However, the phytoplankton population at IS1 had values of $1/\tau_{Q_a \rightarrow PQ}$, E_k, and P^*_{max} that were similar to those observed for the surface populations in the stratified water (Table 3). This suggests that the IS1 population was adapted or acclimated to the highest irradiance experienced during mixing, not to the mean irradiance of the deep-mixed layer (Vincent et al. 1994). Peak daily irradiances were up to six times higher than $E_{k,\text{in situ}}$ for surface-stratified and fully mixed populations, but were approximately equal to $E_{k,\text{in situ}}$ for SCM populations.

Discussion

Spectral dependence of parameters—The spectral dependence of E_k and σ_{PSII} must be taken into account (1) for the calculation of nonspectral parameters including $1/\tau_{PSII}$ (Eq. 6); (2) when comparing parameters measured using different techniques (Fig. 5b); or (3) when investigating relations with in situ light fields (Fig. 7c). However, to simplify the remainder of the discussion, we only discuss spectral dependence where necessary, noting that our conclusions are robust to the normalization wavelength for σ_{PSII}.

Antenna structure and taxonomy—Consistent with other recent field data (Moore et al. 2005), species composition appeared to dominate the observed spatial variability in σ_{PSII}. Additionally, the lack of vertical gradients within the euphotic zone argues against interpreting changes in σ_{PSII} as an acclimation mechanism for these populations (Table 2, Fig. 7b). We conclude that the functional absorption cross-section is a taxonomically (genetically) controlled adaptive parameter within the system at the time of year studied. This conclusion is consistent with a recent extensive laboratory study that showed large interspecific variability and small intraspecific variability of σ_{PSII} across a range of taxa (Suggett et al. 2004). Differences in σ_{PSII} among taxa appears to be principally related to the proportion and type of accessory pigment within the PSII antenna, with package effects probably also important for larger cells (Suggett et al. 2004; Moore et al. 2005). The result suggests that caution should be applied when attributing variability in σ_{PSII} for natural communities to acclimative physiological variability or nutrient stress, unless taxonomic variability can be eliminated as a contributing factor.

Changes in other parameters related to antenna structure could also be interpreted in terms of taxonomic shifts. Both the Chl a:RCII ratio and the proportion of absorbed irradiance transferred to PSII was determined largely by the

relative proportion of eukaryotes and prokaryotes within the community.

It is not clear to what extent the taxonomic variability observed in the current study is related to selective pressure on antenna structure. Although multiple factors will govern species competition, given the diversity of marine autotrophs (Falkowski and Raven 1997), it is likely that the structure of the light-harvesting complex could play some role. For any given total cellular light absorption, a species with a larger PC : Chl *a* ratio and hence higher σ_{PSII} (Table 2, Fig. 5a) will require fewer RCIIs. Selective pressure between taxa with different σ_{PSII} may thus be related to the availability of resources for the production of large antenna pigment–protein complexes (principally requiring nitrogen) versus the greater resources (including iron) required for synthesis of reaction centers (Behrenfeld et al. 1998). Strzepek and Harrison (2004) recently suggested that such a mechanism has resulted in genotypic variability in the ratio of RCII to PSI reaction centers between coastal and oceanic diatoms. For the current study, higher values of σ_{PSII} for shelf break populations (Tables 1 and 2, Fig. 5) may thus have represented an adaptation to conditions of lower resource availability for reaction center synthesis.

Electron turnover and acclimation—Correlated declines of E_k and P^*_{max} as a function of increased OD for stratified stations were consistent with physiological acclimation to low irradiance (MacIntyre et al. 2002). The common relations between E_k (or P^*_{max}) and OD between sites, despite some taxonomic variability, suggest that these vertical gradients primarily result from acclimation. The acclimation mechanism was likely an increase of photosynthetic pigment per cell in the SCM compared to the surface. The ratio of red (chlorophyll) fluorescence to cell volume (F : Cell vol) was a factor of 2.1 ± 0.3 and 3 ± 0.8 larger for the SCM as opposed to the surface at stations CS1 and CS3 respectively (not shown). These differences were of comparable magnitude to the changes in E_k (Table 3), consistent with adjustment of chlorophyll : cell and chlorophyll : C ratios being the factor responsible for the acclimation response (MacIntyre et al. 2002).

Variability in $1/\tau_{PSII}$, rather than σ_{PSII}, dominated changes in E_k (and P^*_{max}), strongly suggesting that acclimation to low light involved an increase in the number of reaction centers, as opposed to an increase in antenna size (Figs. 6, 7). We conclude that the increased numbers of reaction centers for the SCM populations resulted in a higher ratio of RCII : cell (or RCII to carbon fixation capacity) and hence slower turnover rates, as previously observed for *Dunaliella tertiolecta* (Sukenik et al. 1987).

It is reasonable to assume that the maximum achievable (i.e., intrinsic) rate of Q_a through PQ electron transport, 1–1.6 ms^{-1} (Crofts and Wraight 1983; Falkowski and Raven 1997), would not be affected by an acclimation mechanism involving synthesis of RCIIs. The achieved rate of Q_a reoxidation ($1/\tau_{Q_a \to PQ}$, Fig. 6a) of 0.3 to 0.9 ms^{-1} was below this maximum value for many of the populations studied, suggesting that there was an excess PSII capacity (Behrenfeld et al. 1998; Kaňa et al. 2002).

Similar magnitudes and significant correlations between estimates of $1/\tau_{PSII}$ and $1/\tau_{Q_a \to PQ}$ indicated a balance between processes downstream and upstream of the PQ pool (Fig. 6a). The achieved Q_a reoxidation rate appeared to be governed by downstream processes and ultimately constrained by the capacity for carbon fixation to reoxidize the PQ pool, which then oxidizes Q_a (Kolber and Falkowski 1993; Cleland 1998; Kaňa et al. 2002). Photoacclimation thus appeared to change both $1/\tau_{Q_a \to PQ}$ and $1/\tau_{PSII}$, which is consistent with recent models (Geider et al. 1998), particularly if the signal for this process resides within the redox state of the PQ pool (Escoubas et al. 1995).

A degree of balance between electron transport and carbon fixation supports the potential use of active fluorescence for productivity estimation (Kolber and Falkowski 1993; Suggett et al. 2001). Electron transport appeared to be a reasonable indicator of carbon fixation in this system where photoacclimation was the dominant cause of variability in the *P* versus *E* curve. This is the so-called ''E_k-dependent'' behavior identified by Behrenfeld et al. (2004). Electron transport and carbon fixation may be less tightly coupled in a system where ''E_k-independent'' variability is large (Behrenfeld et al. 2004). Further work is clearly desirable to investigate the covariation of $1/\tau_{Q_a \to PQ}$ and $1/\tau_{PSII}$ under a variety of growth conditions.

Photoacclimation and environmental forcing in stratified water columns—The optimal light-harvesting strategy depends on balancing light absorption with carbon fixation, while minimizing the potential loss of photosynthetic performance due to photodamage. Photoacclimation reduced cellular pigment and increased $1/\tau_{PSII}$ in the surface relative to the SCM. This mechanism was effective in shifting the value of $E_{k,\text{in situ}}$ (cf. Eq. 6) to partially track changes in ambient irradiance (Fig. 7c). For SCM populations $E_{k,\text{in situ}}$ was typically fourfold higher than the estimated mean daily irradiance, while for surface populations these two values were more equal. Thus, peak irradiances significantly exceeded $E_{k,\text{in situ}}$ for surface populations, indicating a greater potential for RCII damage and hence photoinhibition.

In situ profiles using the submersible FRR fluorometer indicated significant antenna NPQ at stratified sites (Fig. 4e), as evidenced by midday decreases of around 30–40% in surface values of the functional absorption cross-section (σ'_{PSII}) relative to the dark adapted value (σ_{PSII}) (Olaizola et al. 1994; Falkowski and Raven 1997). A greater capacity for antenna NPQ in surface populations was consistent with the higher NPC : Chl *a* ratio (Table 2). Decreased σ'_{PSII} could thus have increased the in situ value of E_k by 40–70% (Eq. 6); however, peak irradiances would still exceed $E_{k,\text{in situ}}$ (Olaizola et al. 1994). As outlined above, excess PSII capacity, which can raise $1/\tau_{PSII}$ (Fig. 6) and thus E_k further (Eq. 6), could have maintained maximum carbon fixation rates even if some of the RCIIs were photoinhibited (Behrenfeld et al. 1998; Kaňa et al. 2002).

Photoacclimation and environmental forcing in mixed water columns—The acclimation or adaptation to relatively high light that we observed at the mixed station in the Irish Sea (IS1) is consistent with the data of Vincent et al. (1994). In contrast, the field data of Behrenfeld et al. (1998) indicate

acclimation to irradiances below the mean value in a shallow (i.e., optically thin) mixed layer where the depth of mixing was likely less than the 1% light level. Although acclimation to lower irradiance can result in a lower initial $1/\tau_{PSII}$ and hence a higher excess PSII capacity (Behrenfeld et al. 1998), such a strategy may also increase the probability of any individual RCII being reduced in bright light and thus the potential for photodamage (Baroli and Melis 1998). In contrast, we can also speculate that a larger population of reduced RCIIs might increase NPQ, offsetting the potential for photodamage. Increased NPQ may result from quenching within a proportion of the closed RCIIs (Krause and Weis 1991). Additionally, when a large proportion of RCIIs are reduced, energy dissipation by quenchers within the antenna may be enhanced by the increased probability of the excitons populating the antenna (Horton et al. 1996). Resolution of such issues awaits further clarification of the roles of different NPQ mechanisms in situ.

Recent evidence suggests that q_I may contribute significantly to decreases in the quantum yield of chlorophyll fluorescence in situ and hence the overall level of NPQ (Morrison 2003). Although we could not fully dismiss long-lived quenching at IS1, we observed no diel variability in the maximum PSII quantum yield (F'_v/F'_m) at depths >40 m, despite vigorous mixing throughout the water column, arguing against a major role for q_I. Observed reversible antenna NPQ was minimal at IS1 with σ'_{PSII} <10% lower than σ_{PSII} (Fig. 4f), despite relatively high levels of NPC (Table 2). Lower antenna quenching in situ may result from mixing being faster than the timescale for complete NPQ induction or relaxation (Moore et al. 2003). The lowest values of σ_{PSII} were observed at the IS1 station (Table 2, Fig. 5a), consistent with the phytoplankton at this site being adapted to minimize overexcitation of PSII and potential photodamage (Park et al. 1997; Baroli and Melis 1998; Behrenfeld et al. 1998). Such adaptation would be particularly important if reversible antenna NPQ is not an effective strategy in this vigorously mixed environment (Moore et al. 2003). Additionally, a lower σ_{PSII} allows for a lower $1/\tau_{PSII}$ at any given E_k (Eq. 6), consistent with observations in the mixed and surface-stratified waters (Figs. 6a, 7c). Lower $1/\tau_{PSII}$, combined with an adaptively lower σ_{PSII}, could result in a larger excess PSII capacity, without a corresponding increase in the probability of RCII photodamage (Baroli and Melis 1998). Thus, the lower functional absorption cross-sections in phytoplankton adapted to deep mixed coastal waters may reduce q_I and the potential for photodamage to adversely affect carbon fixation (Park et al. 1997; Baroli and Melis 1998; Behrenfeld et al. 1998).

For the region studied, mixed waters are also characterized by excess micro- and macronutrients. High nutrient availability potentially negates any disadvantage, such as a higher cellular iron quota, incurred by taxa with lower σ_{PSII} having to synthesize greater numbers of RCIIs for a given amount of total cellular absorption (Strzepek and Harrison 2004).

The energetic cost of repairing damaged RCIIs may be less than that of not acclimating to low light under many conditions (Raven 1994). However, given sufficiently vigorous mixing, the rapid transport of photodamaged cells from the surface to low irradiance at depth may increase the cost of photoinhibition to the point where acclimation or adaptation to high light becomes the optimal strategy (Behrenfeld et al. 1998). Understanding photoacclimation and adaptation strategies in mixed layers is likely to require knowledge of the timescales and mechanisms for the different components of NPQ induction and relaxation and an understanding of vertical cell movements by turbulent motion. Mechanistic understanding of interactions between NPQ, photoinhibition, and photoacclimation will also be required. These remain formidable research objectives.

Environmental forcing generates selective pressures on the genotypes present within an ecosystem, resulting in changes in taxonomic composition. Environmental forcing can also drive physiological (phenotypic) responses that may ameliorate or exacerbate these selective pressures. Such physiological acclimation can affect selection by modifying the energetic and resource requirements for growth. Gradients in forcing can thus be accompanied by changes in both acclimation state and community composition. This study provides new insights into the functioning of the shelf sea ecosystem in terms of both acclimation and adaptation. Photosynthetic parameters related to the makeup of the pigment antenna, specifically the PSII antenna, showed most variation in the horizontal, largely as a result of changes in community composition within the shelf sea region studied. Conversely, rates of maximum electron transport, carbon fixation, and light saturation intensity varied in the vertical as a result of photoacclimation to the light gradient in stratified waters. This acclimation response was dominated by changes in RCII : cell rather than PSII antenna size.

References

BARLOW, R. G., R. MANTOURA, M. A. GOUGH, AND T. W. FILEMAN. 1993. Pigment signatures of the phytoplankton composition in the northeastern Atlantic during the 1990 spring bloom. Deep-Sea Res. II **40:** 459–477.

BAROLI, I., AND A. MELIS. 1998. Photoinhibitory damage is modulated by the rate of photosynthesis and by the photosystem II light-harvesting chlorophyll antenna size. Planta **205:** 288–296.

BEHRENFELD, M. J., O. PRASIL, M. BABIN, AND F. BRUYANT. 2004. In search of a physiological basis for covariations in light-limited and light saturated photosynthesis. J. Phycol. **40:** 4–25.

———, ———, Z. S. KOLBER, M. BABIN, AND P.G. FALKOWSKI. 1998. Compensatory changes in Photosystem II electron turnover rates protect photosynthesis from photoinhibition. Photosynth. Res. **58:** 259–268.

BIDIGARE, R. R., M. E. ONDRUSEK, J. H. MORROW, AND D. A. KIEFER. 1990. In vivo absorption properties of algal pigments. SPIE **1302 (Ocean Optics X):** 289–302.

CLELAND, R. E. 1998. Voltammetric measurement of the plastoquinone redox state in isolated thylakoids. Photosynth. Res. **58:** 183–192.

CROFTS, A. R., I. BAROLI, D. KRAMER, AND S. TAOKA. 1993. Kinetics of electron-transfer between Q(A) and Q(B) in wild-type and herbicide-resistant mutants of *Chlamydomonas reinhardtii*. Z. Naturforsch. **48c:** 259–266.

———, AND C. A. WRAIGHT. 1983. The electrochemical domain of photosynthesis. Biochim. Biophys. Acta **726:** 149–185.

CULLEN, J. J., AND R. F. DAVIS. 2003. The blank can make a big

difference in oceanographic measurements. Limnol. Oceanogr. Bull. **12:** 29–35.

CULLEN, J. J., AND J. G. MACINTYRE. 1998. Behaviour, physiology and the niche of depth-regulating phytoplankton, p. 559–580. *In* D. M. Anderson, A. D. Cembella, and G. M. Hallegraeff [eds.], Physiological ecology of harmful algal blooms. Springer-Verlag.

DUBINSKY, Z., P. G. FALKOWSKI, AND K. WYMAN. 1986. Light harvesting and utilisation by phytoplankton. Plant Cell Physiol. **27:** 1335–1349.

ESUCOUBAS, J., M. LOMAS, J. LAROCHE, AND P. G. FALKOWSKI. 1995. Light intensity regulation of cab gene expression is signalled by the redox state of the plastiquinone pool. Proc. Natl. Acad. Sci. USA **92:** 10237–10241.

FALKOWSKI, P. G. 1980. Light-shade adaptation in marine phytoplankton, p. 99–119. *In* P. G. Falkowski [ed.], Primary productivity in the sea. Plenum Press.

———, AND J. LAROCHE. 1991. Acclimation to spectral irradiance in algae. J. Phycol. **27:** 8–14.

———, AND T. G. OWENS. 1980. Light shade adaptation: Two strategies in marine phytoplankton. Plant Physiol. **66:** 632–635.

———, AND J. A. RAVEN. 1997. Aquatic photosynthesis. Blackwell.

GEIDER, R. J., H. L. MACINTYRE, AND T. M. KANA. 1998. A dynamic regulatory model of phytoplankton acclimation to light nutrients and temperature. Limnol. Oceanogr. **43:** 679–694.

HORTON, P., A. V. RUBAN, AND R. G. WALTERS. 1996. Regulation of light harvesting in green plants. Annu. Rev. Plant Physiol. Plant Mol. Biol. **47:** 655–684.

KAŇA, R., D. LAZAR, O. PRASIL, AND J. NAUS. 2002. Experimental and theoretical studies on the excess capacity of photosystem II. Photosynth. Res. **72:** 271–284.

KOLBER, Z., AND P. G. FALKOWSKI. 1993. Use of active fluorescence to estimate phytoplankton photosynthesis in situ. Limnol. Oceanogr. **38:** 1646–1665.

———, O. PRASIL, AND P. G. FALKOWSKI. 1998. Measurements of variable chlorophyll fluorescence using fast repetition rate techniques: Defining methodology and experimental protocols. Biochim Biophys Acta **1367:** 88–106.

———, K. D. WYMAN, AND P. G. FALKOWSKI. 1990. Natural variability in photosynthetic energy conversion efficiency: A field study in the Gulf of Maine. Limnol. Oceanogr. **35:** 72–79.

———, J. Zehr, and P. G. Falkowski. 1988. Effects of growth irradiance and nitrogen limitation on photosynthetic energy conversion in photosystem II. Plant Physiol. **88:** 923–929.

KRAUSE, G. H., AND E. WEIS. 1991. Chlorophyll fluorescence and photosynthesis: The basics. Annu. Rev. Plant Physiol. Plant Mol. Biol. **42:** 313–349.

LANEY, S. R. 2003. Assessing the error in photosynthetic properties determined by fast repetition rate fluorometry. Limnol. Oceanogr. **48:** 2234–2242.

LEWIS, M. R., E. P. W. HORNE, J. J. CULLEN, N. S. OAKEY, AND T. PLATT. 1984. Turbulent motions may control phytoplankton photosynthesis in the upper ocean. Nature **311:** 49–50.

LONG, S. P., S. HUMPHRIES, AND P. G. FALKOWSKI. 1994. Photoinhibition of photosynthesis in nature. Annu. Rev. Plant Physiol. Plant Mol. Biol. **45:** 633–662.

MACINTYRE, H. L., T. M. KANA, T. ANNING, AND R. J. GEIDER. 2002. Photoacclimation of photosynthesis irradiance response curves and photosynthetic pigments in microalgae and cyanobacteria. J. Phycol. **38:** 17–38.

MAUZERALL, D., AND N. L. GREENBAUM. 1989. The absolute size of a photosynthetic unit. Biochim. Biophys. Acta **974:** 119–140.

MOORE, C. M., M. I. LUCAS, R. SANDERS, AND R. DAVIDSON. 2005. Basin-scale variability of phytoplankton bio-optical characteristics in relation to bloom state and community structure in the Northeast Atlantic. Deep Sea Res. I. **52:** 401–419.

———, AND OTHERS. 2003. Physical controls on phytoplankton physiology and production at a shelf sea front: A fast repetition-rate fluorometer based field study. Mar. Ecol. Prog. Ser. **259:** 29–45.

MORRISON, R. J. 2003. In situ determination of the quantum yield of phytoplankton chlorophyll *a* fluorescence: A simple algorithm, observations and a model. Limnol. Oceanogr. **48:** 618–631.

OLAIZOLA, M., J. LAROCHE, Z. KOLBER, AND P. G. FALKOWSKI. 1994. Non-photochemical quenching and the diadinoxanthin cycle in a marine diatom. Photosynth. Res. **41:** 357–370.

PARK, Y. I., W. S. CHOW, AND J. M. ANDERSON. 1997. Antenna size dependency of photoinactivation of photosystem II in light-acclimated leaves. Plant Physiol. **115:** 151–157.

PERRY, M. J., M. C. TALBOT, AND R. S. ALBERETE. 1981. Photoadaptation in marine phytoplankton: Response of the photosynthetic unit. Mar. Biol. **62:** 91–101.

PRASIL, O., N. ADIR, AND I. OHAD. 1992. Dynamics of photosystem II: Mechanism of photoinhibition and recovery process, p. 295–348. *In* J. Barber [ed.], The photosystems: Structure, function and molecular biology. Elsevier.

———, Z. KOLBER, J. BERRY, AND P. G. FALKOWSKI. 1996. Cyclic electron flow around PSII in vivo. Photosynth. Res. **48:** 395–410.

RAVEN, J. 1994. The cost of photoinhibition to plant communities, p. 449–464. *In* N. R. Baker and J. R. Bowyer [eds.], Photoinhibition of photosynthesis: From molecular mechanisms to the field. BIOS Scientific Publishers.

RICHARDSON, K., BEARDALL, J., AND J. A. RAVEN. 1983. Adaptation of unicellular algae to irradiance: An analysis of strategies. New Phytol. **93:** 157–191.

SHARPLES, J., C. M. MOORE, T. P. RIPPETH, P. M. HOLLIGAN, D. J. HYDES, N. R. FISHER, AND J. H. SIMPSON. 2001. Phytoplankton distribution and survival in the thermocline. Limnol. Oceanogr. **46:** 486–496.

STRZEPEK, R. F., AND P. J. HARRISON. 2004. Photosynthetic architecture differs in coastal and oceanic diatoms. Science **431:** 689–692.

SUGGETT, D., G. KRAAY, P. HOLLIGAN, M. DAVEY, J. AIKEN, AND R. GEIDER. 2001. Assessment of photosynthesis in a spring cyanobacterial bloom by use of a fast repetition rate fluorometer. Limnol. Oceanogr. **46:** 802–810.

———, H. L. MACINTYRE, AND R. J. GEIDER. 2004. Evaluation of biophysical and optical determinations of light absorption by photosystem II in phytoplankton. Limnol. Oceanogr. Methods **2:** 316–332.

SUKENIK, A., J. BENNETT, AND P. G. FALKOWSKI. 1987. Light-saturated photosynthesis-limitation by electron transport or carbon fixation? Biochim. Biophys. Acta. **891:** 205–215.

TASSAN, S., AND G. M. FERRARI. 1995. An alternative approach to absorption measurements of aquatic particles retained on filters. Limnol. Oceanogr. **40:** 1358–1368.

VINCENT, W. F., N. BERTRAND, AND J. J. FRENETTE. 1994. Photoadaptation to intermittent light across the St. Lawrence Estuary freshwater-saltwater transition zone. Mar. Ecol. Prog. Ser. **110:** 283–292.

Received: 10 March 2005
Accepted: 13 September 2005
Amended: 17 October 2005